Original Research Article

Numerical Study of Natural Solutal Convection in an Isoscele Trapezoidal Cavity

ABSTRACT

A numerical study of the natural heat and mass transfer in a cavity with a straight isoscele cross-section containing air is made in this paper. The two inclined side walls are kept in natural convection with the surrounding environment. The upper horizontal wall is subjected to a heat flux of constant density, while the lower one is adiabatic. Under the Boussinesq assumption, the thermodynamic conditions are numerically studied using the unsteady convection equations formulated as a secondary variable of vorticity and a stream function, energy and moisture. The system of equations discretised by the implicit finite difference method is solved by the Thomas algorithm. The results show a flow structure, isotherms and isohumidities dependent on the study parameters. Thus, on one hand, an increase in the inclination angle of the walls is accompanied by an increase in the velocity of the fluid. On the other hand, an increase in the aspect ratio or Lewis number leads to a decrease in the fluid's velocity. The average Nusselt number, which is independent of the Rayleigh number, increases slightly as the inclination angle of the walls decreases. The increase of the Lewis number results in the decrease of the flow velocity components values. It is observed that the maxima values of velocity components were reached for Rayleigh number equal to 7.10^3.

Keywords: Natural convection, isoscele trapezoidal cavity, Boussinesq approximation, critical Rayleigh, Nusselt number, Lewis number

1. INTRODUCTION

Natural convection in cavity is an important problem due to its significant practical applications. In energy related applications, natural convection plays a dominant role in transport of energy for the proper design of enclosures in order to achieve higher heat transfer rates. Some important applications involving this type of heat transfer are air conditioned system in building, furnace and home heating, electronic equipment cooling, drying foods, double pane windows, etc. Increasing of flow dynamic behaviour as fluid velocity and heat transfer performance in this type of systems is an essential topic. Thus, a lot of works are carried out by researchers in the area taking into account the geometric parameters.

The study of thermoconvection in trapezoidal cavities with a single inclined wall has been a subject of several works. Lam et al. [1] studied "experimentally and numerically the natural convection heat transfer in trapezoidal cavity having a hot horizontal base, a cool inclined top and insulated vertical walls. The results showed higher Nusselt number than expected in the range of $8.10^3<Ra<2.10^5$ for inclinations of 0 to 5°. The Nusselt number decreases overally, when the inclination is increased. The proportions of convective heat flow rate into the high side and low side of the cavity were measured and show distinct maxima at particular Rayleigh numbers independently to the top surface inclination angle". Kuyper et al.

[2] investigated “a numerical study on the laminar natural convection flow of air in differentially heated trapezoidal enclosures. Special attention is paid to the applied solution method, using a coordinate-invariant formulation of the transport equations. For Rayleigh numbers between 10^4 and 10^8, results are presented for inclination angles of the isothermal walls from -45° (trapezoidal enclosure) to 0° (square enclosure). The flow and heat transfer in the corners of the enclosure have been shown to be strongly dependent on the intersection angles between the isothermal and adiabatic walls. For trapezoidal enclosure (γ = 45°), the averaged Nusselt number shows a power law dependence on the Rayleigh number of the flow, similar to the relation for a square enclosure (γ = 0°)”. Boussaid et al.[3] studied “the natural convection heat transfer and mass in a trapezoidal cavity heated by the base and cooled by the upper inclined wall. The equations relating to the transport of momentum, energy and concentration are solved by the finite volume method. The results showed flow patterns dependent on the inclination of the top wall. Thus, for low angles of inclination, the flow was of the Rayleigh-Bernard type; besides, for strong inclinations, the flow was more akin to the case of the rectangular cavity heated differentially. The increase in the length of the cavity leads to an increase in the rates of heat and mass transfer”. Acharya et al. [4] investigated “the effect of baffles placed on the inclined upper wall of trapezoidal cavity. The results obtained with air as the working fluid reveal a decrease in heat transfer in the presence of baffles. In general, the heat transfer decreases when the height of the baffles is increased”. Lasfer et al. [5] studied the effect of the side walls inclination of an isocele trapezoidal cavity on the dynamic behaviour and heat transfer in the turbulent regime. For values of δ ranging from 90° to 110°, it was shown that despite the intensification of the flow, the average Nusselt number through both side walls decreases. Similarly, they have shown that the increase of the exchange surface (side walls), caused by the variation of the inclination from δ = 90° decreases the heat transfer, except for the cold wall (for δ between 70° and 90°). They also noticed that the heat transfer gained is greater than that lost, for values of δ between 93.5° and 110° and reciprocally for values of δ between 70° and 93.5°. An unsteady numerical study of double diffusive mixed convection flow in a trapezoidal enclosure with the uniform magnetic field effect applied in negative horizontal is conducted by Borhan Uddin et al. [6]. The transport phenomenon of this problem can be expressed by the coupled governing equation derived from the conservation of mass and momentum along with the energy equation for temperature and concentration. The finite element method (FEM) based on Galerkin weighted residual technique is used to compute the numerical result from these governing equations. The numerical computation is carried out for Lewis number (Le = 0.1–50) and Richardson’s number (Ri=0.1–100). Computed numerical results of mass, temperature and velocity distribution are expressed graphically as iso-concentration lines, isotherm lines and streamlines respectively. Average Sherwood and Nusselt number values are used to show the mass and heat transfer rate from the heated and concentrated surface of the enclosure. It is found from the analysis that mass transfer strongly depends on Lewis number. Esfe et al. [7] investigated “numerically the natural convection heat transfer inside a trapezoidal enclosure filled with carbon nanotube–EG–water nanofluid using variable properties. The bottom and top walls of trapezoidal enclosure are kept at constant temperatures Th and Tc, respectively, while the side walls of the cavity are thermally insulated. The governing equations have been discretized, using the finite volume method and the SIMPLER algorithm. Simulations have been carried out for different aspect ratios, Rayleigh numbers of 10^3–10^6 as well as solid volume fractions of 0.0015, 0.03, and 0.045. The results show that at low Rayleigh number ($Ra < 10^4$), the average Nusselt number decreases with increasing the inclination angle (aspect ratio) at all solid volume fractions. While for $Ra=10^6$, the average Nusselt number increases and then decreases with inclination angle. Moreover, the average Nusselt number increases with increasing Rayleigh number at fixed inclination angle and solid volume fraction”. Benzema et al.[8] presented “a numerical investigation of steady and laminar mixed convection flow within an irregular ventilated enclosure, crossed by Cu–Water Nano

fluid. The bottom wall is maintained at a constant and uniform temperature, whereas the top and the vertical walls are adiabatic. The inclined wall is kept at a lower constant temperature. The governing coupled equations are resolved by the means of the finite volume technique. The results reveal that the flow structure is more sensitive to both Richardson and Reynolds numbers variation. Thus, heat transfer is enhanced by the increase of Richardson and Reynolds numbers".

In the further part of this literature review, we present the work on natural convection in trapezoidal cavities with two inclined walls.Venkatadri et al. [9] studied "a natural convection in two-dimensional laminar incompressible flow in a trapezoidal enclosure with the presence of thermal radiation, motivated by energy systems applications. Heat flow visualization via the method of energy flux vectors (EFVs) is also included. The trapezoidal cavity has an inclined top wall which in addition to the bottom wall is maintained at constant temperature, whereas the remaining (vertical side) walls are adiabatic. The governing partial differential conservation equations are transformed using a vorticity-stream function formulation and non-dimensional variables and the resulting nonlinear boundary value problem is solved using a finite difference method with incremental time steps. A comprehensive parametric study is performed to evaluate the impact of Rayleigh number (buoyancy parameter) and radiation parameter on transport phenomena. The computations indicate that local Nusselt number and velocity are increasing functions of the Rayleigh number and radiation parameter. Significant changes in streamlines, temperature contours and energy streamlines for high Rayleigh number are observed. The energy flux vectors shows that a large eddy is formed within the enclosure which migrates towards the cold wall. Greater thermal buoyancy force accelerates the primary flow, whereas it decelerates the secondary flow". Rostami et al. [10] provided "a review of recent natural convection studies on non-rectangular cavities, free convection depends more on the fluid velocity relative to the forced convection, leading to the opposite effect of some parameters that should essentially enhance rate of heat transfer. Nanoparticle addition, magnetic fields, fins, and porous media may reduce free convection due to the reduction in fluid velocity. Thus, these parameters need more precision and sometimes need the optimization of effective parameters". Ghouizi et al. [11] did "a numerical study of natural convection in a trapezoidal cavity, filled with a nanofluid whose wall containing a square heat source of side dimensionless ε = 0.1.This wall is successively inclined at an angle γ varying from 0 to 60 ° at the most with respect to the horizontal. The upper and lower walls on either side of the heat source are adiabatic while the other walls are subjected to a constant cold temperature. The hydrodynamic and thermal phenomena are described by the equations of Navier-Stokes and energy. The models Brinkman and Wasp are used to describe the thermo-physical properties of the nanofluid (water-Al_2O_3). The finite element method, based on the Galerkin principle, is used to solve the system of partial differential equations. The effect of the angle of inclination of the lower wall for different values of the Rayleigh number on the results obtained, are considered in the form of isotherms, local and average modified Nusselt numbers.The results showed that the rate of heat transfer increases with the increase of the Rayleigh number.The rate of heat transfer increases with increasing angle of inclination of the bottom wall of the cavity which leads to good geometric design, good cooling of the heat source and this is the case for the trapezoidal cavity at the optimal angle of inclination γ = 60°compared to a square cavity of γ = 0°". Dogonchi et al. [12] studied natural convection mode of heat transfer of Al_2O_3-water nanofluid by considering the effects of radiation parameter, porous media, magnetic field, and also the changes in geometry on the Nusselt number and entropy generation (Bejan number) in a crown cavity with a cylinder inside. The flow is considered buoyancy-driven which is under thermal radiation (Rd) and constant magnetic field within the porous media. Dimensionless modes of Navier-Stokes equations are considered as governing equations, and Finite Element Method is used to discretize the equations. The geometry with the best heat transfer performance is the one with the base wavy wall and the cylinder at the left side". Ishak et al**.** [13] made "a numerical analysis of entropy generation and natural

convection in a trapezoidal cavity with an internal solid cylinder filled with Al_2O_3–water nanofluid, using finite difference method. Particular factors have been focused on the effects of Rayleigh number, dimensionless radius of the solid cylinder and nanoparticles of volume fraction on streamlines, isotherms, isentropic, local and average Nusselt numbers. Obtained results have demonstrated that the Rayleigh number and size of the solid cylinder are important control parameters for optimizing heat transfer and Bejan number. Thus, the increase in number of Rayleigh and solid cylinder radius has a significant impact on heat transfer and fluid flow. The average number of Nusselt rises with increasing numbers of Rayleigh. Heat transfer irreversibility dominates the system at smaller Rayleigh numbers, however nanofluid flow irreversibility dominates the system as the number of Rayleigh increases. At smaller radius of solid cylinder and higher nanoparticles volume fraction, the average Nusselt number reaches a maximum". Bilal et al. [14] examined the transfer of heat in cavities embedding fins, as well as the effect of a range of several parameters upon the transmission of energy. The Fourier law is applied to formulate the heat transfer rate inside the fluid flow region. The formulated system describing the problem is non-dimensionalized using similarity transformations. The geometry of the problem comprises a trapezoidal cavity with a non-uniformly heated U-shaped fin introduced at the center of the base of the enclosure. The solution of the non-dimensionalized equations is procured by the Galerkin finite element procedure. It is deduced from the study that ascending magnitude of (Ra) elevates level of kinetic energy and magnitude of heat flux; however, a contrary configuration is encapsulated for the power-law index. This study highlights that the momentum profile and the heat transfer increase by increasing Rayleigh number (Ra) and decline as the viscosity of the fluid increases".

"The double-diffusive convection of two rotating rods inside an infinite-shaped saturated porous cavity filled by a suspension of nano-encapsulated phase change material was investigated numerically using the (ISPH) method" [15]. The cavity includes two rotating rods, (NEPCM) particles, and porous media. The inner left and right rods are located inside the left and right sides of an infinite-shaped cavity. In this work, two types of boundary conditions between the inner rods and outer boundary walls of the cavity are considered. It was found that the location and the strength of the melting-solidification zone are influenced significantly by the variation of the boundary conditions. The average Nusselt and Sherwood numbers are influenced clearly by the variation of the boundary conditions for rods and cavity walls and by increasing the length of the inner rods. Kolsi et al. [16] performed "a numerical investigation on the double diffusive natural convection in a finned solar still using the finite volume method. The 3D vector potential-vorticity formalism is used to eliminate the gradient pressure terms and due to the complex shape of the cavity the blocked-off-region method is adopted. After getting the dimensionless governing equations, they are written in a generalized form then discretized. The effects of the buoyancy ratio, conductivity ratio and Rayleigh number of the flow structure, temperature field and heat and mass transfer are studied. The results show that the increase of conductivity ratio and Rayleigh number leads to an enhancement of the heat and mass transfer".

A review of the literature shows strong studies on the heat and mass transfer within the non-rectangular cavities. However, thermosolutal natural convection across an isoscele trapezoidal cavity with an imposed heat flux at the top wall has received less attention. This configuration is similar to the air draft zone of the "ASUTO" charcoal stove.The main objective of this paper is to study the effect of geometric parameters (aspect ratio, inclination angle of sidewalls) and other parameters such as Rayleigh number, Lewis number and Nusselt number on the flow structure, isotherms, isoconcentration lines of moisture and specifically on the velocity components values in the trapezoidal cavity for it further application to the air draft in "ASUTO" charcoal stove.

2. GEOMETRY AND MATHEMATICAL FORMULATION

2.1. Geometry

The geometry of the problem considered is illustrated in Fig.1. It is an isoscele trapezoidal cavity which represents the air draft zone of the "ASUTO" charcoal stove. Indeed, the "ASUTO" cooking stove is one of the most used charcoal cooking stoves in Africa, particularly in TOGO. It has a primary air draught zone that promotes the charcoal combustion process in its combustion chamber. A cross-section of this air draft zone located at the bottom of its combustion chamber has the shape of an isoscele trapezoidal cavity. The side walls, inclined at an angle α to the vertical, are maintained in natural convection with the ambient air. A constant heat flow is imposed on the upper horizontal wall. The lower horizontal wall is assumed to be adiabatic.

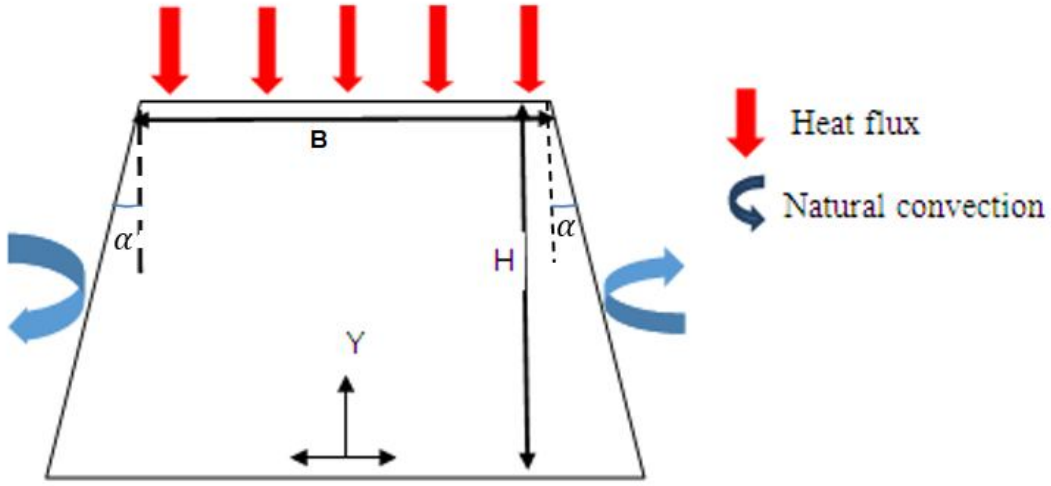

Fig.1. Geometrical model

2.2. Mathematical formulation

2.2.1. Assumptions

To simplify the physical problem, the following assumptions have been made:

- the flow is assumed to be two-dimensional;
- the fluid is Newtonian and incompressible;
- the flow regime is considered as laminar;
- the heat transfer by radiation is negligible;
- the Soret and Dufour cross effects are negligible;
- Viscous dissipation and the pressure term in the heat equation are negligible.

- the physical properties of the air inside the cavity are assumed to be constant except the density of fluid assumed to obey to the Boussinesq approximation. It consists in considering the variations of the density negligible at the levels of all the terms of the equations, except the gravity term. The variation of ρ as a function of temperature and concentration is given by the following formula:

$$\rho = \rho_0[1 - \beta_T(T - T_0) - \beta_c(C - C_0)] \#(1)$$

Where T_0 and C_0 the temperature and the reference concentration, β_T the coefficient of thermal expansion at constant pressure, β_C the coefficient of solutal expansion at constant pressure, ρ_0 is the density of fluid at T_0.

2.2.2. Governing equations in dimensional form

Based on the above assumptions, governing equations representing the conservation of mass, momentum, energy and concentration are expressed in dimensional form as follows:

$$\frac{\partial u}{\partial x} + \frac{\partial v}{\partial y} = 0 \quad (1)$$

$$\frac{\partial u}{\partial t} + u\frac{\partial u}{\partial x} + v\frac{\partial u}{\partial y} = -\frac{1}{\rho}\frac{\partial (p-p_0)}{\partial x} + \nu\left[\frac{\partial^2 u}{\partial x^2} + \frac{\partial^2 u}{\partial y^2}\right] \quad (2)$$

$$\frac{\partial v}{\partial t} + u\frac{\partial v}{\partial x} + v\frac{\partial v}{\partial y} = -\frac{1}{\rho}\frac{\partial (p-p_0)}{\partial y} + \nu\left[\frac{\partial^2 v}{\partial x^2} + \frac{\partial^2 v}{\partial y^2}\right] + g\beta_T(T-T_0) + g\beta_C(C-C_0) \quad (3)$$

$$\frac{\partial T}{\partial t} + u\frac{\partial T}{\partial x} + v\frac{\partial T}{\partial y} = \alpha\left[\frac{\partial^2 T}{\partial x^2} + \frac{\partial^2 T}{\partial y^2}\right] \quad (4)$$

$$\frac{\partial C}{\partial t} + u\frac{\partial C}{\partial x} + v\frac{\partial C}{\partial y} = D\left[\frac{\partial^2 C}{\partial x^2} + \frac{\partial^2 C}{\partial y^2}\right] \quad (5)$$

In order to overcome the difficulty posed by the boundary conditions to be imposed on the pressure to solve the momentum equations, the equations of motion (2) and (3) are transformed into the equation (6) using stream function-vorticity formulation:

$$\frac{\partial w}{\partial t} + u\frac{\partial w}{\partial x} + v\frac{\partial w}{\partial y} = \nu\left[\frac{\partial^2 w}{\partial x^2} + \frac{\partial^2 w}{\partial y^2}\right] + g\beta_T\frac{\partial T}{\partial y} + g\beta_C\frac{\partial c}{\partial y} \quad (6)$$

With :

$$u = \frac{\partial \psi}{\partial y}; \quad v = -\frac{\partial \psi}{\partial x} \quad \text{and} \quad \omega = \frac{\partial v}{\partial x} - \frac{\partial u}{\partial y} = -\left(\frac{\partial^2 \psi}{\partial x^2} + \frac{\partial^2 \psi}{\partial y^2}\right) \quad (7)$$

The associated initial conditions can be written as:

$$u = v = 0; T = T_0; c = c_0 \quad (8)$$

The boundary conditions are :

-on the top horizontal wall:

$$u = v = 0, \lambda\frac{\partial T}{\partial y} = q; \; c = 0 \quad (9)$$

-on the bottom horizontal wall:

$$u = v = 0, \frac{\partial T}{\partial y} = 0; \; \frac{\partial C}{\partial x} = 0 \quad (10)$$

-on the inclined side walls:

$$u = v = 0, -\lambda\frac{\partial T}{\partial n} = h(T_P - T_a); \; \frac{\partial C}{\partial n} = 0 \quad (11)$$

where n is the outgoing normal to the wall.

2.2.3. Equations of the mathematical model in dimensionaless form

Dimensionless variables used are as follow:

$$X = \frac{x}{H};\ Y = \frac{y}{H};\ U = \frac{u}{\left(\frac{\alpha}{H}\right)};\ V = \frac{v}{\left(\frac{\alpha}{H}\right)};\ \tau = \frac{t\alpha}{H^2};\ \Omega = \frac{\omega H^2}{\alpha};\ \theta = \frac{\lambda(T-T_0)}{qH};\ C = \frac{c}{c_0} \quad (12)$$

The dimensionless governing equations representing the conservation of mass, momentum, energy and concentration under the above assumptions are given as:

$$\frac{\partial \Omega}{\partial \tau} + U\frac{\partial \Omega}{\partial X} + V\frac{\partial \Omega}{\partial Y} = \mathrm{P_R}\left(\frac{\partial^2 \Omega}{\partial X^2} + \frac{\partial^2 \Omega}{\partial Y^2}\right) + R_{aT}P_r\frac{\partial \theta}{\partial X} + R_{aM}P_r\frac{\partial C}{\partial X} \quad (13)$$

$$\frac{\partial^2 \Psi}{\partial X^2} + \frac{\partial^2 \Psi}{\partial Y^2} = -\Omega \quad (14)$$

$$\frac{\partial \theta}{\partial \tau} + U\frac{\partial \theta}{\partial X} + V\frac{\partial \theta}{\partial Y} = \left(\frac{\partial^2 \theta}{\partial X^2} + \frac{\partial^2 \theta}{\partial Y^2}\right) \quad (15)$$

$$\frac{\partial C}{\partial \tau} + U\frac{\partial C}{\partial X} + V\frac{\partial C}{\partial Y} = \frac{1}{L_e}\left(\frac{\partial^2 C}{\partial X^2} + \frac{\partial^2 C}{\partial Y^2}\right) \quad (16)$$

The problem studied is subjected to the initial and boundary conditions in the dimensionless form.

The initial conditions are as follow:

$$U = V = 0;\ \theta = 0;\ \Omega = 0;\ C = 1 \quad (17)$$

The boundary conditions are expressed as:

-on the top horizontal wall:

$$U = V = 0;\ \frac{\partial \theta}{\partial Y} = 1, \Omega = \frac{\partial U}{\partial Y};\ \Psi = 0;\ C = 0 \quad (18)$$

-on the bottom horizontal wall:

$$U = V = 0;\ \frac{\partial \theta}{\partial Y} = 0;\ \Omega = -\frac{\partial^2 \Psi}{\partial Y^2};\ \Psi = 0;\ \frac{\partial C}{\partial Y} = 0 \quad (19)$$

-on the inclined side walls:

$$U = V = 0;\ -\frac{\partial \theta}{\partial n} = \frac{h}{\lambda}\theta;\ \Omega = \frac{\partial V}{\partial X} - \frac{\partial U}{\partial Y};\ \Psi = 0;\ \frac{\partial C}{\partial n} = 0 \quad (20)$$

where n is the outgoing normal to the wall.

3. NUMERICAL METHOD AND VALIDATION

3.1. Numerical method

To obtain the numerical solution of equations (3) to (6), finite difference method (FDM) was used. This method is chosen because it is stable, of rapid convergence, accurate, and simple to solve partial differential equations [17,18]. By applying FDM, the continuous domain is discretized and the differential terms of the equation are converted into a linear algebraic equation. Additionally, dependent variables are considered only at discrete points. The systems of algebraic equations obtained is tri-diagonal matrix and has been solved using Thomas algorithm with a Gauss–Seidel iteration technique. The unknown variable Φ was calculated iteratively until the following criteria of convergence was fulfilled:

$$\sum \left| \frac{\Phi^n(i,j) - \Phi^{n-1}(i,j)}{\Phi^n(i,j)} \right| \leq 10^{-8} \quad \#(11)$$

where n represents the current iteration, Φ represents temperature, humidity, stream function or vorticity. The numerical code used for the solution of our problem has been developed with the FORTRAN 95 language. The steady state is reached when the difference between all variables from the previous iteration to the current iteration is less than 10^{-6}.

3.2. Grid independency

The transport equations are discretized on a uniform mesh. The inclined walls are approximated by a staircase shape which, by densifying the mesh, reduces significantly the error generated by this shape. Details of this approach can be found in Mahmoudi et al. [19] and Ouyahia et al. [20]. Table 1 groups the grid independency tests performed to monitor the sensitivity of the results to the mesh size for Pr = 0.71 and α =30. It appears that for a mesh size of 81 × 51 (along the X and Y directions respectively), the numerical solution is only slightly affected by the mesh size.

Table 1. Sensitivity of results to mesh size for side wall inclination angle of α = 30°

Mesh (Y ×X)	61 × 41	71 × 41	81×51	121 × 81	121 × 91
Mean Nusselt	7.86033	6.51071	6.14529	6.15519	6.13493

For Pr = 0.71 and α =15, the 81 × 51 mesh is still retained as giving slightly affected numerical solutions. This is shown in the table 2.

Table 2. Sensitivity of results to mesh size for side wall inclination angle of α =15°

Mesh (Y × X)	61 × 51	71 × 41	81 × 51
Mean Nusselt	8.24529	6.49616	6.48356

3.3. Validation

To study the validation of this simulation, the current results is compared with those of the literature. We qualitatively compared the flow structure and isotherms (Fig.2) obtained by Aydin et al. [21] and our results for the case of mixed convection in a square cavity with moving walls and heated from below in the middle of the side. The analysis of Fig.2 shows a great similarity between the streamlines and isotherms, obtained by our computational code and those of Aydin et al. [21]. Further validation is done by comparing quantitatively (figure 3) the transverse profile of the vertical component of the flow velocity at the vertical midplane of the cavity for Ri=2 and for Ri=10. It is also presented in Fig.4 the profile of local Nusselt number versus the abscissa for Ri=10. It can be noted in Fig.3 and 4 a good agreement between our results and those of Aydin et al. [21]. Indeed, the numerical accuracy on the local Nusselt number and vertical dimensionless velocity component at the vertical midplane of the cavity is less than 3%.

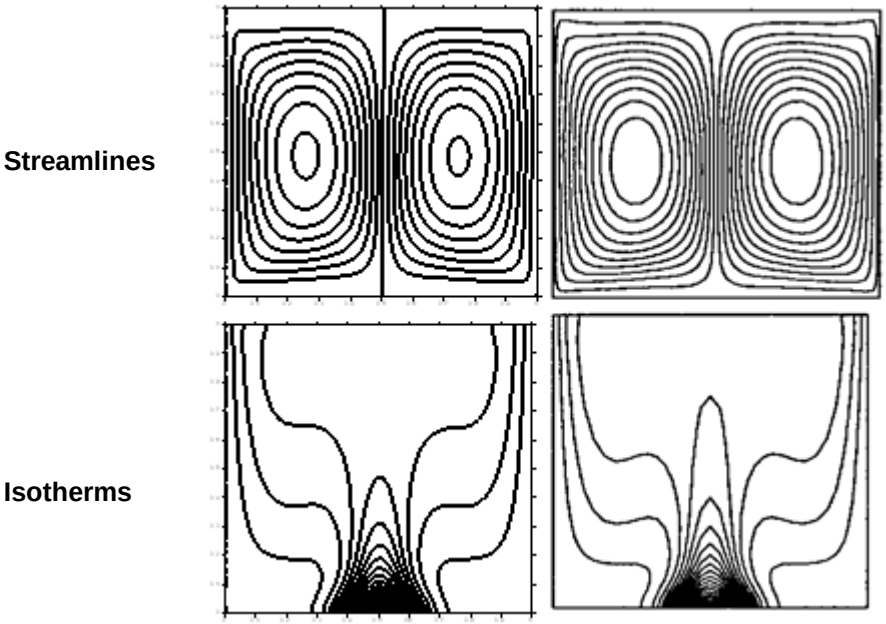

Fig.1. Comparison of streamlines lines and isotherms of the present work (a) with that of Aydin et al. [21].

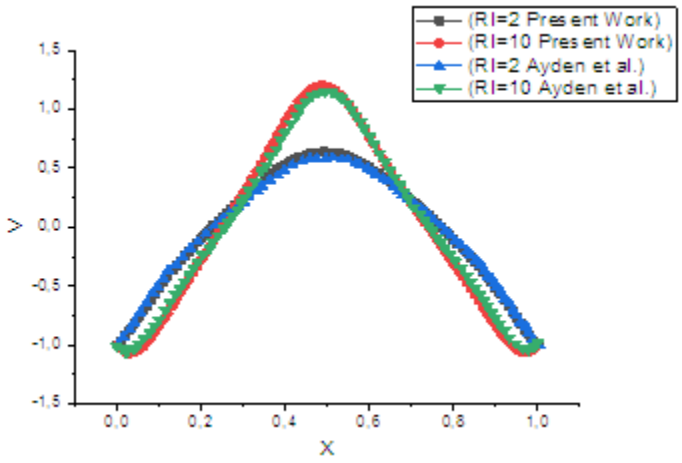

Fig.2. Comparison of the nondimensional vertical velocity profiles at the vertical midplane of the cavity for Ri=2 and for Ri=10 (results of Aydin et al. [21] and present work)

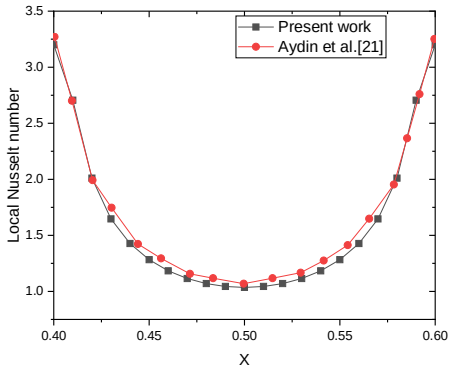

Fig.3. Comparison of local Nusselt number of the present work and that of Aydin et al. [21] for Ri=10

4. Results and discussions

4.1. Flow structure in the cavity

The flow structure is depicted by Fig.5. The cavity is symmetrical with respect to its vertical axis, which justifies the obtaining of a flow structure formed by two symmetrical cells, whose strength depends on the Rayleigh number Ra. For a Rayleigh number equals to 7.10^2, the two flow cells are very weak. This situation expresses a weak flow dominated by a thermal diffusion choked by a stable vertical temperature stratification. In this situation where the upper wall is hot and the lower wall is cold, even in the case of a large thermal Rayleigh number, the temperature gradient tends to keep the fluid particles stationary, so the temperature gradient has a stabilizing role. Each cell rises through the axis of symmetry, then faces the inclined side wall in natural convection through which it undergoes heat exchange with the surrounding medium, moves horizontally along the lower adiabatic wall toward the axis of symmetry.

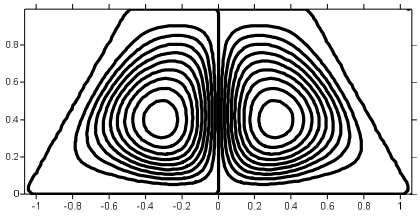

Fig.5. Distribution of streamlines for Pr=0.71 ; F=1 ; Ra=7.10^2

4.2. Temperature fields

The temperature field shown in Fig.6 is similar to the case of a rectangular cavity heated from below, referred to as the Rayleigh Bernard instability. The isotherms separate from the top wall symmetrically on either side of the cavity symmetry axis. They are parallel to the inclined wall demonstrating the predominance of heat transfer by conduction over convection heat transfer on the near walls. They are deformed and stratified on both sides of the axis of symmetry of the cavity.

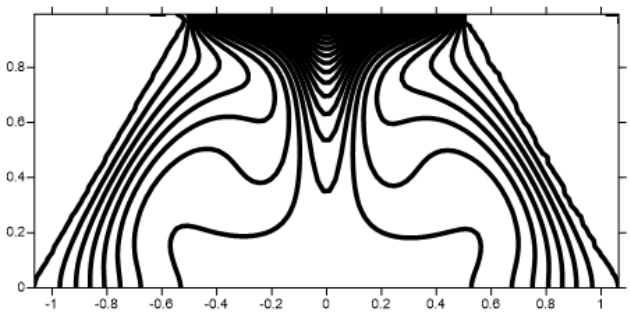

Fig.6. Distribution of isothermal lines for Pr=0.71 ; F=1 ; Ra=7.10^2

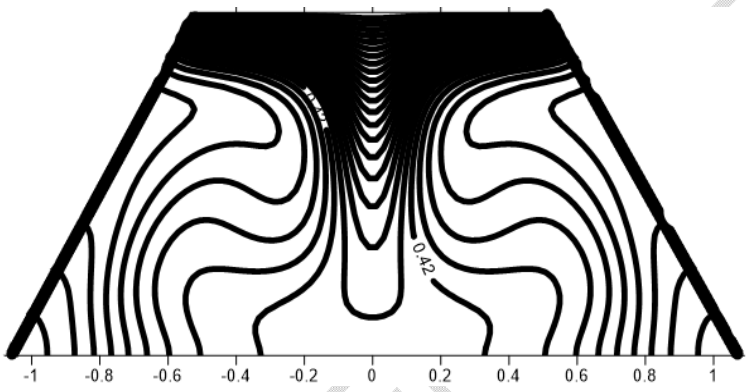

Fig.7. Distribution of moisture isovalues contours for Pr=0.71; F=1; Ra=7.10^2

4.3. Moisture fields

The humidity field shown in Fig.7 is identical to that of the temperatures, except that the lines of iso-concentration are perpendicular to the sloping walls due to the impermeability boundary condition imposed on them. Like the isotherms, the humidity lines are parallel and tight to the heated horizontal wall, which indicates a dominant heat transfer by conduction with a symmetrical stratification on both sides of the symmetry axis of the cavity.

4.4. Model sensitivity analysis

4.4.1. Effect of the side walls inclination

Fig.8 shows the flow structures, isotherms and iso-humidity lines in the cavity for different angles of inclination of the walls, namely 30°, 22.5° and 15°. We notice qualitatively that the flow lines, the isotherms and the iso-humidities are not modified. These lines lengthen in one case as in the other in order to fit the new configuration offered by the variation of the inclination. On the other hand, the lengthening of the streamlines in the cavity causes a loss in intensity. Indeed, Fig.9 presenting the profiles of the velocities U and V in the cavity for the different angles of inclination considered, shows a decrease of the extremums reached by the flow velocity. The decrease of the inclination angle of the walls is thus accompanied by a decrease in the intensity of the flow in the cavity. This same observation is observed for the moisture profile in the cavity. Fig.10 (b) shows the longitudinal moisture profile in the cavity at one quarter or three quarters of its width (for symmetry, the profile at one quarter and three quarters of the width are identical). It shows that the moisture in the cavity

decreases with the angle of inclination of the walls implying a more intense evaporation at 15° than at 30°.Indeed, Fig.10 (a) shows the longitudinal temperature profiles in the cavity as a function of different wall tilt angles. As the inclination angle decreases, the temperature in the cavity increases. This results in a tightening of the isotherms at the near inclined side walls as the hot upper horizontal; the stratification of isothermal lines observed for an inclination of 30° decreases and disappears in the upper half of the cavity. The conduction mode of transfer dominates convection one. In addition, the isohumidity lines widen with decreasing tilt, a consequence of greater mass transfer by convection.

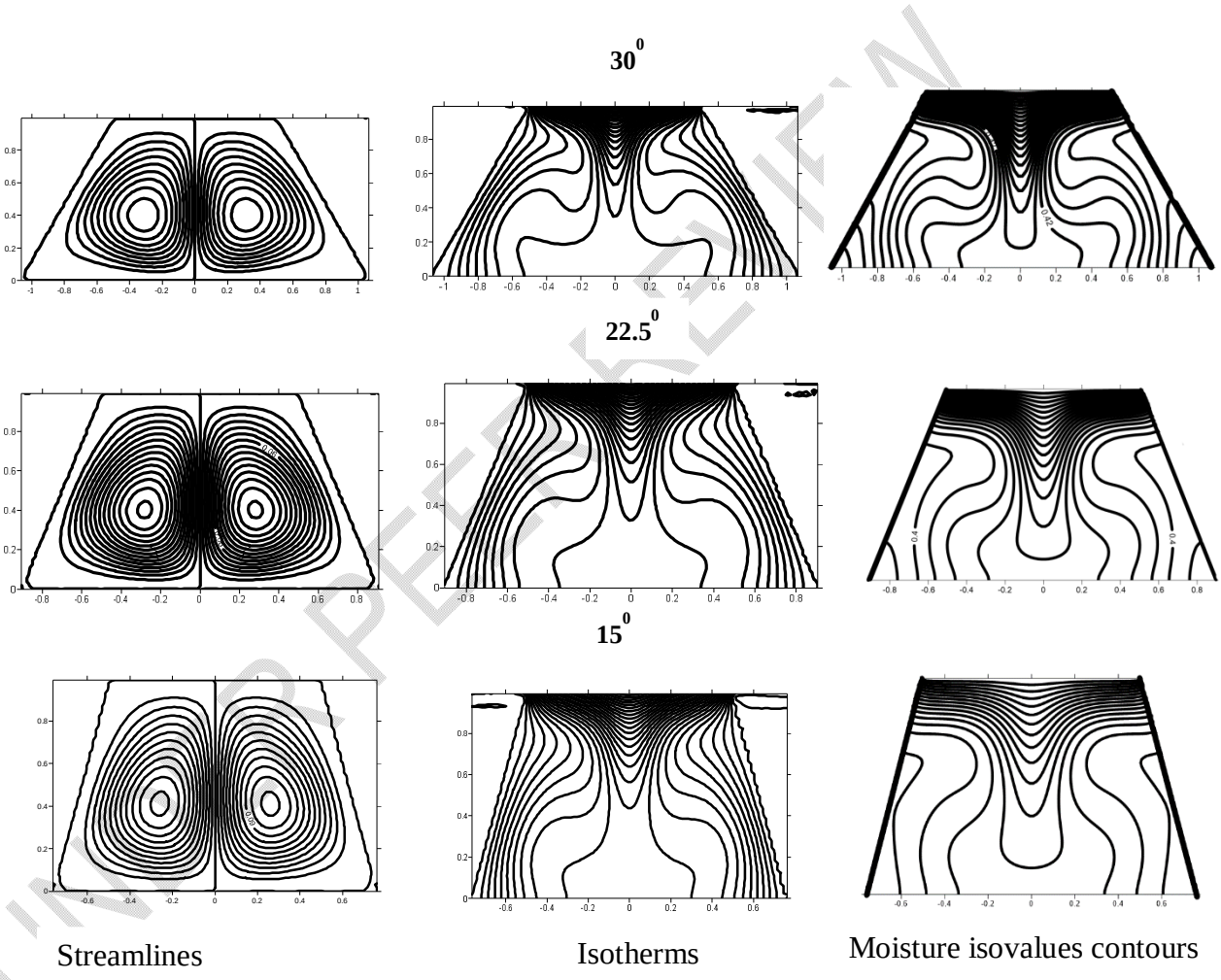

Fig.8. Effect of wall slope on streamlines, isotherms and moisture isovals

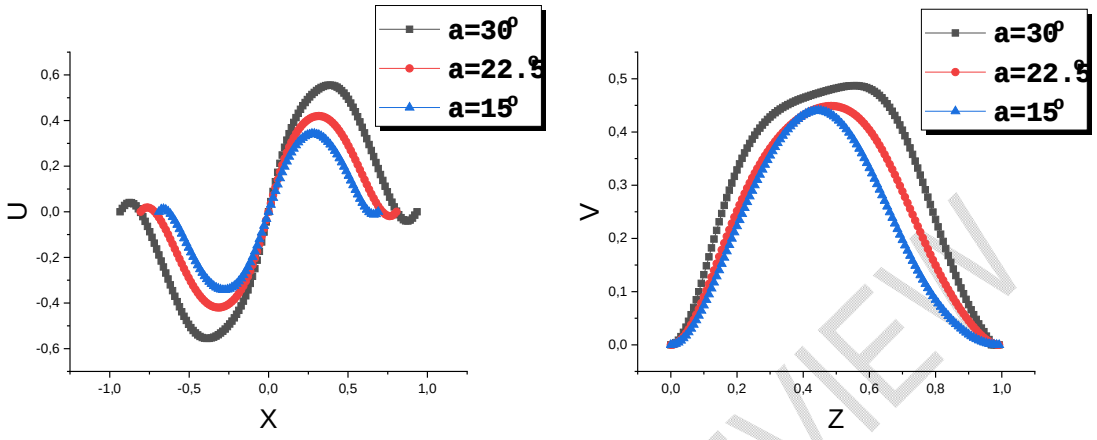

Fig.9. Longitudinal and transverse velocity profiles for various wall slopes

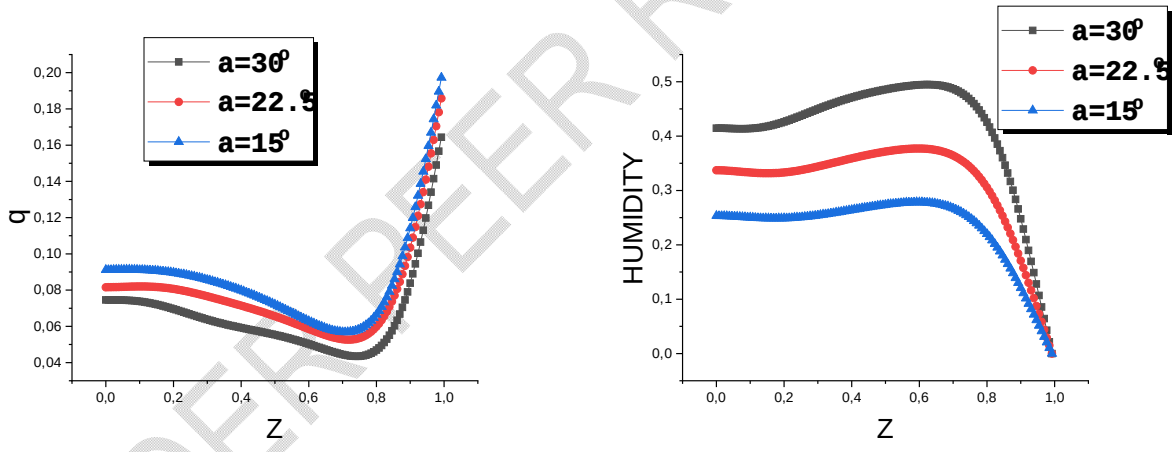

Fig.10. Longitudinal temperature (a) and moisture (b) profiles for various wall slopes

4.4.2. Effect of the geometric aspect ratio F

Fig.11 shows the flow structure, isotherms and isovalues of moisture in the cavity for three values of the geometric aspect ratio (F=H/B). The geometric aspect ratio is the ratio of the height H of the cavity to its diameter B: F=H/B. As the aspect ratio increases, the structure of the flow changes and the size of the rotating cells increases until they occupy the cavity. This increase in the size of the rotating cells is accompanied by a decrease in the dynamic field strength. This is revealed in Fig.12 showing the transverse and longitudinal velocity profiles for geometric aspect ratio F=1, F=1.5 and F=2. Indeed, the maximum values of its velocity components are multiplied by three for aspect ratio going from F=1.5 to F=1. The increase in the height of the cavity is accompanied by a decrease in the air velocity in the cavity.

The distribution of the isotherms agrees with that of the streamlines. However, they are parallel and dense in the vicinity of the hot upper wall. A uniformity towards the bottom of the cavity is observed for F=1.5. This shows that increasing the height of the cavity decreases its heat transfer capacity towards the base of the cavity. The evaporation of moisture from the air in the cavity therefore decreases as the geometric aspect ratio increases from 1 to 2. Thus, the isohumidity lines are tighter in the cavity for an aspect ratio F=1, demonstrating the predominance of heat transfer by conduction, than for F=1.5.

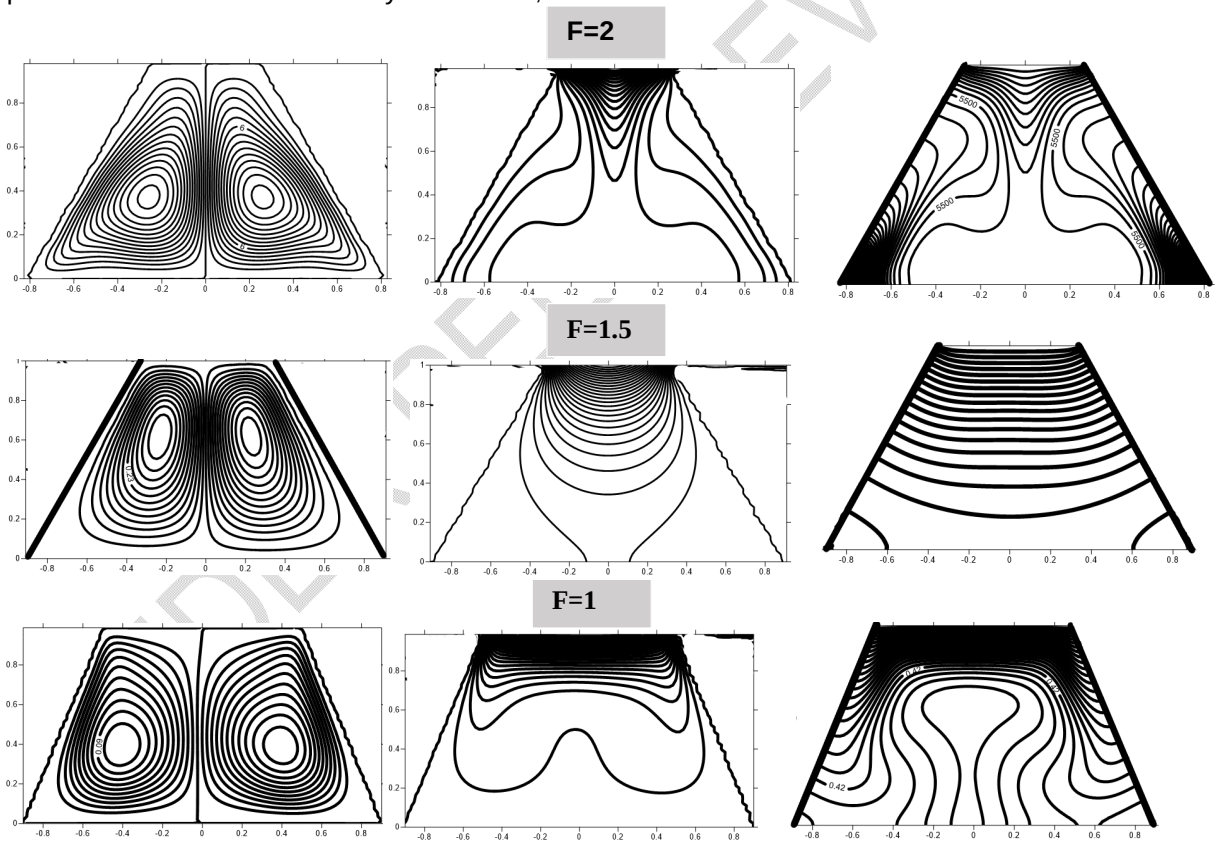

Fig.11. Influence of the geometrical form factor on streamlines, isotherms and isovals of humidity

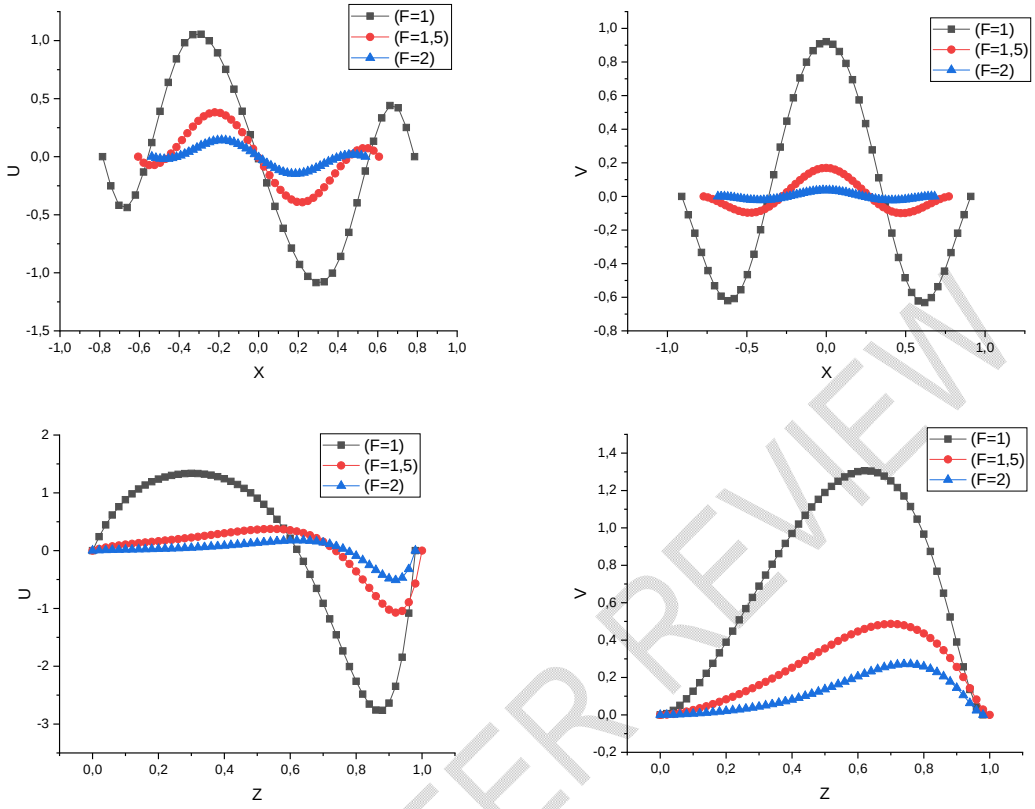

Fig.12. Longitudinal and transverse velocity profiles for form factors F=1, F=1.5 and F=2

4.4.3. Effect of the Rayleigh number

Fig.13 shows the structure of the streamlines, isotherms and isohumidities for the Rayleigh numbers Ra=7.10^2, 7.10^3 and 7.10^4. A modification of the flow structure downwards can be observed from a value of the Rayleigh number equal to 7.10^3 (Ra=7.10^3). At this value of the thermal Rayleigh number, the flow velocity in the cavity reaches its extremum. This is shown in Fig.14: the longitudinal as well as transverse velocity profiles presented at different heights (1/4 and ¾) and then at different widths (¼ and ¾) for distinct values of the thermal Rayleigh number shows velocities framed by the Ra=7.10^3 case. As described above, even in the case of a large thermal Rayleigh number, the temperature gradient tends to keep the fluid particles immobile, explaining the existence of the critical Rayleigh (Ra=7.10^3) at which the velocity of the fluid particles reaches its maximum. It is obvious that this situation where the thermal diffusivity is greater than the mass diffusivity will have a consequence on the temperature and concentration distribution where we observe a clear dominance of the thermal stratification in the core of the cavity, compared to the solute diffusivity where the concentration gradient is weaker in the middle and intense near the walls.

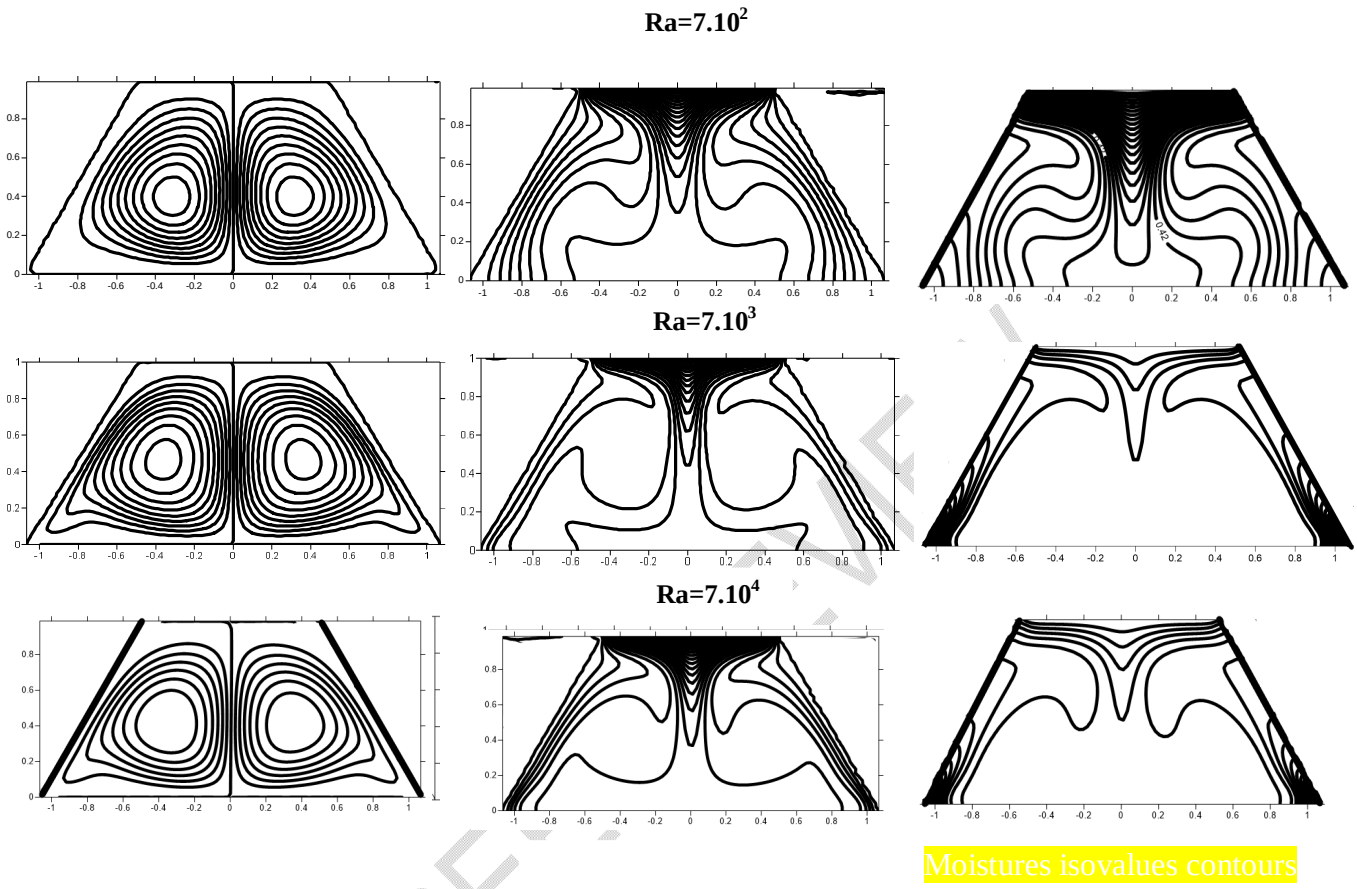

Fig.13. Effect of Rayleigh number on streamlines, isotherms and moisture isovalues

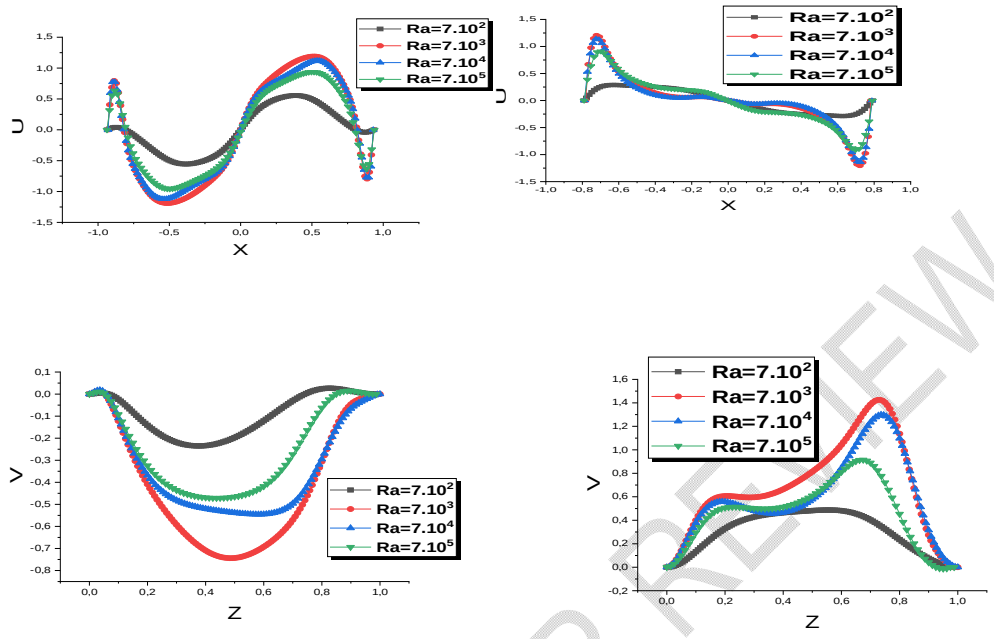

Fig.14. Longitudinal and transverse velocity profiles as a function of thermal Rayleigh number

4.4.4. Effect of the Lewis number

It is presented in Fig.15 the structures of the flow, isotherms and isohumidity for the critical Rayleigh number ($Ra=7x10^3$) and for different values of the Lewis number (Le=1, 10 and 50). The Lewis number determines the ratio of the thermal diffusivity to the solutal diffusivity. For Lewis number equal to unity (Le=1), we observe a weak solutal stratification in the form of a plume pushed back by a thermal stratification dominating the core of the cavity. The flow structure is two-celled, symmetrical with respect to the vertical axis of symmetry of the cavity. As the Lewis number increases to 10, the two-cell flow remains with a downward shift of the eye. A deformation of the streamlines in the lower corners of the cavity is noticed. A strong solutal stratification takes place in the cavity, the isotherms on the other hand are parallel to the inclined walls with slight deformation. Heat transfer is mainly by conduction. The flow becomes almost stagnant and multicellular with more than 4 cells for Le=50. The velocity profiles presented in Fig.16 show an almost stationary flow for Le=50. The amplitude of the air velocity decreases as the Lewis number increases from 1 to 10 and then to 50. The origin of this oscillatory flow can be attributed to instabilities of a thermosolutal nature caused by an amplification of the concentration perturbations. As a result, patches of uniformly concentrated fluid appear on the iso-moistures. These disturbances affect the velocity through the coupling mechanism and thus have an impact on heat and mass transfer. Thus, the maximum value of the velocity decreases when the Lewis number increases.

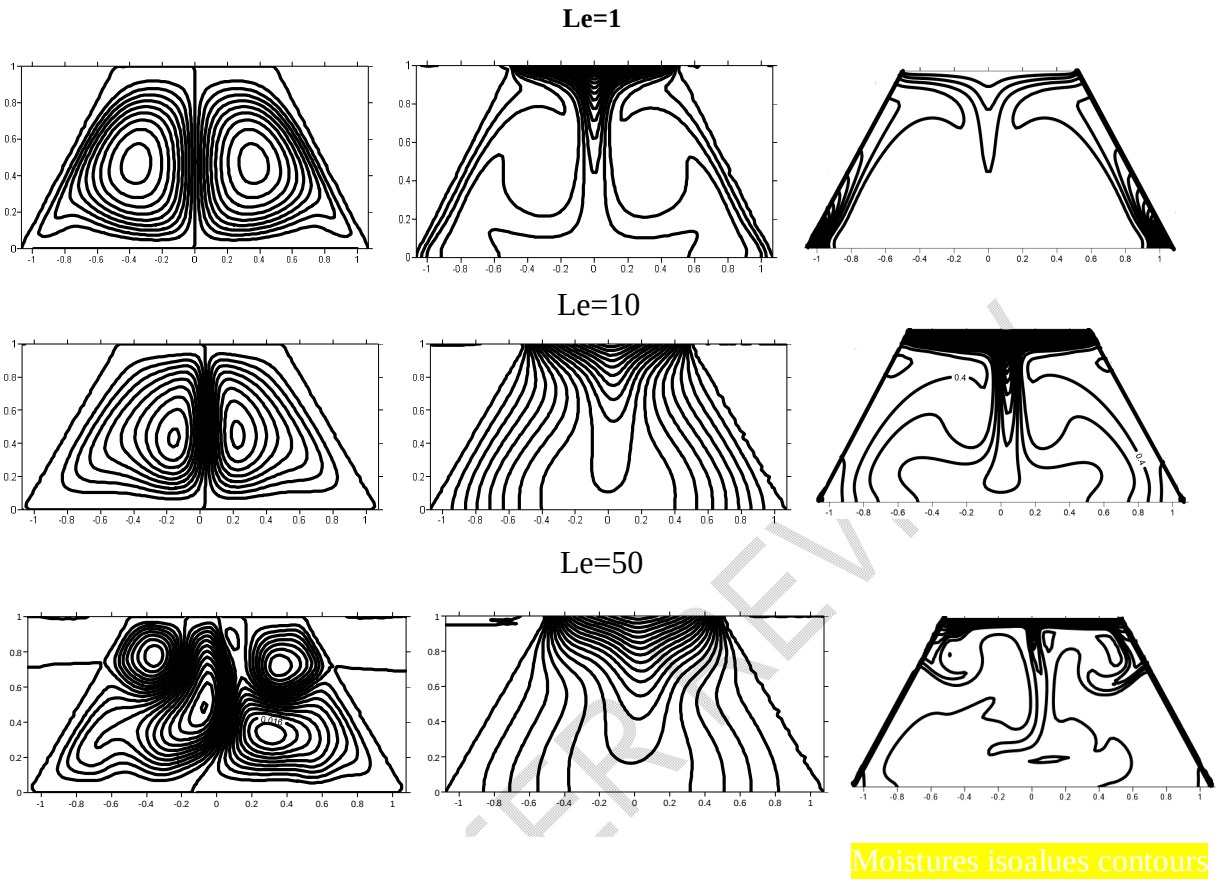

Fig.15. Effect of Lewis number on the Stream lines, Isotherms and Moisture isovals.

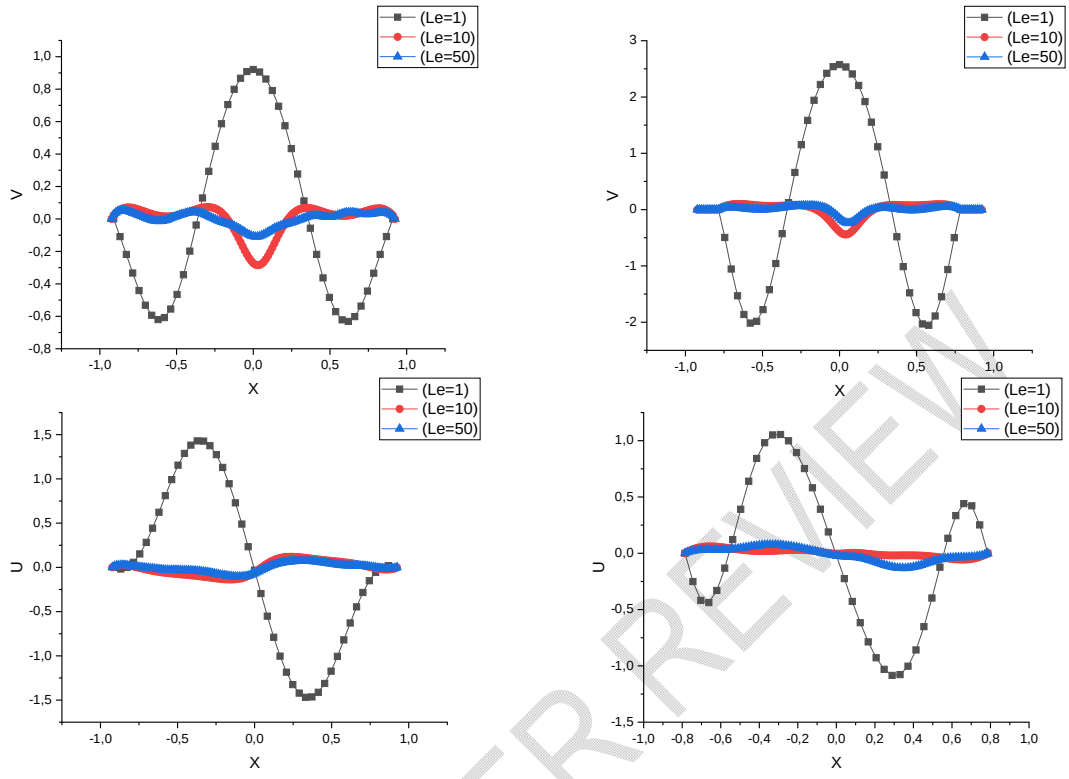

Fig.16. Transverse and longitudinal velocity profiles for Le=1, Le=10 and Le=50.

4.4.5. Effect of the Nusselt number

The Nusselt number is a dimensionless number used to characterize the type of heat transfer between a fluid and a wall. It relates the heat transfer by convection to the heat transfer by conduction. The higher the number is, the more heat transfer by convection predominates over heat transfer by conduction. Fig.17 presents the effect of walls inclination angle on the local Nusselt (a) and average Nusselt number (b).

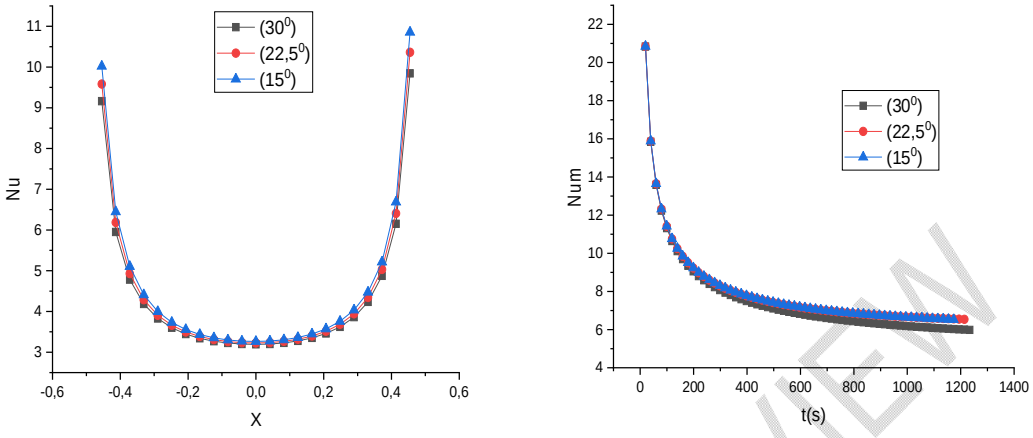

(a)

Fig.17. Effect of walls inclination angle on the local Nusselt (a) and average Nusselt number (b)

In general, there is a slight increase in the average Nusselt (Fig.17 b) or local Nusselt number at the steady state (Fig.17 a) as the wall tilt decreases. This demonstrates an increase in the transfer rate through the active wall with decreasing tilt angle.
Fig.18 shows in (a) the local Nusselt number when the steady state is reached and in (b) the time variation of the average Nusselt number for different values of the thermal Rayleigh number: Ra=7.10^2, Ra=7. 10^3 and Ra= 7.10^4.

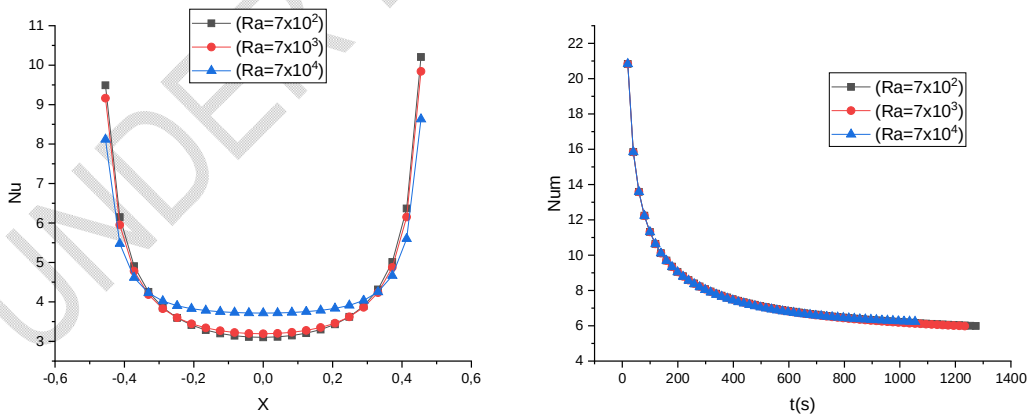

(a) (b)

Fig.18. Effect of the Rayleigh number on the local Nusselt and average Nusselt number

It can be seen from Fig.18(a) that the minimum of the local Nusselt number increases with the increase of the thermal Rayleigh number when the steady state is reached. On the other hand, the maxima reached towards the angular corners of the active wall vary inversely. This makes the time average value of the Nusselt number independent of the value of the thermal Rayleigh number (Fig.18b). Furthermore, the smaller the Rayleigh number is, the longer it takes for the permanent regime to be established.

5. CONCLUSION

A numerical study of heat and mass transfer in natural convection inside a trapezoidal cavity is investigated. The finite difference method was used to solve the governing equations and comparisons with previously published works were performed. A good agreement with the results was found. From current study, the following results are drawn:

-a decrease in the aspect ratio result in the increase of the velocity components values;
-a decrease in the inclination angle leads to the increase of the heat transfer rate and to the decrease of the velocity components values;
-when the Lewis number increases, the flow velocity components values decrease;
-the maxima values of velocity components were reached for Rayleigh number equal to 7.10^3.

REFERENCES

1. Lam SW, Gani R, Symons J. Experimental and Numerical Studies of Natural Convection in Trapezoidal Cavities. J. Heat Transf. 1989;111(2):372–377. doi: 10.1115/1.3250687.
2. Kuyper RA, Hoogendoorn CJ. Laminar natural convection flow in trapezoidal enclosures. Numer. Heat Transf. Part Appl. 1995;28(1):55–67. doi: 10.1080/10407789508913732.
3. Boussaid M, Mezenner A, Bouhadef M. Convection naturelle de chaleur et de masse dans une cavite trapezoidale. Int. J. Therm. Sci.1999;38:363-371.
4. Acharya FM. Natural convection in trapezoidal cavities with baffles mounted on the upper inclined surfaces. Numer. Heat Transf. Part Appl. 2000;37(6):545–565. doi: 10.1080/104077800274082.
5. Lasfer K, Bouzaiane M, Lili T. Etude numérique de la convection naturelle turbulente dans une cavité trapézoïdale. In JITH 2007, 2007.
6. Uddin MB, Rahman MM, Khan MAH, Saidur R, Ibrahim TA. Hydromagnetic double-diffusive mixed convection in trapezoidal enclosure due to uniform and nonuniform heating at the bottom side: Effect of Lewis number. Alex. Eng. J., 2016;55(2): 1165–1176. doi: 10.1016/j.aej.2016.03.035.
7. Esfe MH, Arani AAA, Yan WM, Ehteram H, Aghaie A, Afrand M. Natural convection in a trapezoidal enclosure filled with carbon nanotube-EG-water nanofluid. Int. J. Heat Mass Transf. 2016;92:76–82
8. Benzema M, Benkahla YK, Labsi N, Brunier E, Ouyahia SE. Numerical mixed convection heat transfer analysis in a ventilated irregular enclosure crossed by Cu–water nanofluid. Arab. J. Sci. Eng. 2017;42(11):4575–4586.
9. Venkatadri K, Anwar Bég O, Rajarajeswari P, Ramachandra Prasad V. Numerical simulation of thermal radiation influence on natural convection in a trapezoidal enclosure: Heat flow visualization through energy flux vectors. Int. J. Mech. Sci. 2020; 171:105391. doi: 10.1016/j.ijmecsci.2019.105391.
10. Rostami S. A Review on the control parameters of natural convection in different shaped cavities with and without nanofluid. Processes.2020;8(9)1011.

doi: 10.3390/pr8091011.
11. Ghouizi J, Nabou M, Elmir M, Douha M, Berramdane M. Numerical Simulation of Natural Convection in A Cavity Filled with A Nanofluid Who's Wall Containing the Heat Source Is Inclined. J. Adv. Res. Fluid Mech. Therm. Sci. 2020;76(1):1–16.
doi: https://doi.org/10.37934/arfmts.76.1.116.
12. Dogonchi AS, Sadeghi MS, Ghodrat M, Chamkha AJ, Elmasry Y, Alsulami R. Natural convection and entropy generation of a nanoliquid in a crown wavy cavity: Effect of thermo-physical parameters and cavity shape. Case Stud. Therm. Eng. 2021;27: 101208.
doi: 10.1016/j.csite.2021.101208.
13. Ishak MS., Alsabery AI, Hashim I. Entropy generation and natural convection of nanofluids in a trapezoidal cavity having an innersolid cylinder. J. Phys. Conf. Ser. 2021;1988(1):012012.
doi: 10.1088/1742-6596/1988/1/012012.
14. Bilal S, Rehman M, Noeiaghdam S, Ahmad H, Akgül A. Numerical analysis of natural convection driven flow of a non-newtonian power-law fluid in a trapezoidal enclosure with a U-shaped constructal. Energies. 2021;4(17):5355.
doi: 10.3390/en14175355.
15. Aly AM, Hussein AK, Younis O, Alsedais N, Kolsi L. Double-diffusive convection of two rods in a novel cavity saturated by porous media and suspended by nano-encapsulated phase change materials. Waves in Random and Complex Media. 2022;
DOI: 10.1080/17455030.2022.2100001
16. Kolsi L, Ghachem K, Larguech S, AlNemer G. Numerical investigation of the double diffusive convection in 3D trapezoidal solar still equipped with conductive fins. Mathematics. 2022; 10:2115. https://doi.org/10.3390/math10122115
17. Özişik MN, Orlande HRB, Colaço MJ, Cotta RM. Finite difference methods in heat transfer. CRC Press; 2nd edition, 2017.
https://doi.org/10.1201/9781315121475
18. LeVeque RJ. Finite Difference Methods for Ordinary and Partial Differential Equations: Steady-State and Time-dependent Problems. Society for Industrial and Applied Mathematics; 1st edition, 2007.
19. Mahmoudi AH, Pop I, Shahi M Talebi F. MHD natural convection and entropy generation in a trapezoidal enclosure using Cu–water nanofluid. Comput. Fluids. 2013; 72:46–62
doi: 10.1016/j.compfluid.2012.11.014.
20. Ouyahia SE, Benkahla YK, Labsi N. Numerical study of the hydrodynamic and thermal proprieties of titanium dioxide nanofluids trapped in a triangular geometry. Arab. J. Sci. Eng. 2016;41(5)1995–2009
doi: 10.1007/s13369-016-2055-0.
21. Aydin O, Yang WJ. Mixed convection in cavities with a locally heated lower wall and moving sidewalls. Numerical Heat Transfer, Part A: Applications: An International Journal of Computation and Methodology. 2000;37(7):695-710
http://dx.doi.org/10.1080/104077800274037.

NOMENCLATURE

B : lower length of the trapezoidal cavity, m
c : concentration $mol.l^{-1}$
C : dimensionless concentration $C=c/c_0$
F : aspect ratio (H/B)
g : acceleration due to gravity, $m.s^{-2}$
G_r : Grashof number $G_r= g.\beta_T.qH^4 / v^2\lambda$
h_c : side wall convective coefficient

H : height of the trapezoidal cavity, m
Le : Le Lewis number
P : dimensionless pressure
Pr : Prandtl number
q : thermal flux, $W.m^{-2}$
Ram : Solutal Rayleigh number
Ra_T : Thermal Rayleigh number: $Ra_T=GrP_r$
t : time (s)
T : temperature, K
T_0 : initial temperature of the air, K
u : x component of velocity (m)
U : x component of dimensionless velocity
v : y component of velocity (m)
V : y component of dimensionless velocity
X : dimensionless distance along x coordinate
Y : dimensionless distance along y coordinate

Greek symbols

α : angle of inclination of the side walls (°)
β : volume expansion coefficient, K^{-1}
θ : dimensionless temperature $\theta=(T-T_0)/(qh/\lambda)$
λ : thermal conductivity, $W.m^{-1} K^{-1}$
ν : kinematic viscosity, $m^2 s^{-1}$
τ : dimensionless time $\tau=tu_0/H$
ψ : stream function